

# INFLUENCE OF CATHODIC PROTECTION IMPRESSED CURRENTS ON AAR EXPANSION OF CONCRETE CONTAINING REACTIVE AGGREGATES

Ahmad Shayant, Aimin Xu† and Ross Pritchard\*

† ARRB Group, Melbourne, Victoria, Australia

\* Queensland Department of Main Roads, Brisbane, Queensland, Australia

## Abstract

Impressed current cathodic protection (CP) is an effective method of mitigating corrosion damage to chloride-contaminated reinforced concrete structures. This process generates OH ions through the cathodic reaction and increases the OH concentration in the concrete around the steel bars, which can promote AAR when the concrete contains reactive aggregates and cause further expansion and cracking.

Laboratory studies in the past two decades, using small concrete specimens and relatively high levels of CP current, have confirmed that CP currents can enhance AAR expansion of concrete. In this study, AAR-affected reinforced columns (300x300x1100 mm), were subjected to three levels of CP (5, 10 and 20 mA/m<sup>2</sup>), and their expansion monitored.

Results show that increasing CP currents caused increased AAR expansion. It is recommended that the AAR susceptibility of the concrete, and consequences of increased expansion, be evaluated before the application of impressed current CP systems.

**Keywords:** AAR, Corrosion, Cathodic protection, Impressed current, Expansion

## 1 INTRODUCTION

Corrosion of steel reinforcement in reinforced concrete structures is one of the major deterioration mechanisms for coastal structures subjected to chloride attack. This problem leads to loss of steel section in concrete and induces major cracking and spalling of cover concrete which involves significant maintenance costs, and can compromise the structural integrity of the elements concerned.

The traditional patch repair technique is only temporarily effective and needs to be repeated. Consequently, it is not a cost effective option. A more effective remedial option is the application of impressed current cathodic protection (CP), which suppresses the steel corrosion through inhibiting the corrosion reactions. However, it is known that application of CP increases the alkalinity of concrete around the reinforcement, which could lead to enhancement of alkali-aggregate reaction (AAR), if the concrete contains reactive aggregate [1-5].

Although a current density of 20 mA/m<sup>2</sup> caused only slight AAR expansion in specimens [4], large currents in the range of 1 - 8 A/m<sup>2</sup>, usually used for chloride extraction and desalination, caused significant AAR expansion, even with alkali contents below the threshold of reactivity [5]. The latter observed a “pessimum” effect in the relationship between total charges passed and induced expansion, and cautioned against using high current densities and long durations in chloride extraction or desalination practices. The pessimum effect was also noted [6] for CP current densities in the range of 25 - 200 mA/m<sup>2</sup> at 50mA/m<sup>2</sup> and was attributed to the formation of very fluid, non-expansive gel at high current densities.

Enhanced AAR expansion and reductions in the mechanical properties and load capacity of reinforced concrete has also been reported, where CP has been used [7, 8]. In contrast, the electrochemical re-alkalisation of carbonated concrete [9], using a current of 1A/m<sup>2</sup> and a total charge of 500 ± 50 Ah/m<sup>2</sup>, reportedly decreased the expansion of carbonated concrete.

More recent studies on concrete prisms [10-11] found that the risk of increased expansion depended on the type of aggregate, the alkalinity of concrete, and the magnitude of CP current. At the pessimum current density of 25 mA/m<sup>2</sup>, the increase in expansion amounted to about 20% compared to the case of no CP current. The increase in expansion caused by CP currents was also verified for larger experimental columns subjected to immersion in salt water [12].

The concern is that the augmentation of alkalinity by CP current could exacerbate the AAR expansion and cracking, the extent of which depends on the magnitude of CP current employed. In practice, current levels of 10-25 mA/m<sup>2</sup> are common, the higher level being for the commissioning and the lower levels for maintenance, although it is reported that “hot spots” can develop in some zones, where the current density exceeds the intended level [7].

This study, using CP current levels which are used in practice (5, 10 and 20 mA/m<sup>2</sup>), would clarify the risk of CP application to concrete elements containing reactive aggregate, with and without chloride contamination, and whether it could adversely affect the AAR expansion and cracking in cathodically protected concrete elements.

## **2 EXPERIMENTAL WORK**

### **2.1 Specimens**

The specimens used in this work were six experimental reinforced columns, measuring 300 x 300 x 1100 mm. Details of their manufacture and curing regimes have previously been published in a study of alkali-reactivity potential of some concrete piles [13]. The concrete used in their manufacture had a cement content of 450 kg/ m<sup>3</sup>, and alkali content of 6.3 kg/ m<sup>3</sup>. Three columns contain a highly reactive aggregate (Hr) and the other three a slowly-reactive aggregate (Lr). Reinforcement details in the columns are presented in Figure 1, amounting to a reinforcement ratio of 1.4%. The steel surface area in the specimens is estimated to be about 3000 cm<sup>2</sup>. Embedded concrete strain gauges allow measurement of expansion in the cover concrete and in the centre of columns in the transverse direction. Longitudinal expansion is restrained by the longitudinal steel bars, and is expected to be much smaller.

Two columns were cured at 80°C (Ht) for 8 hours, three hours after casting (note possibility of delayed ettringite formation, DEF), and the other four at ambient temperature of about 20-23 °C (N). Some specimens were half immersed in tap water (W) and some in salt solution containing 3.5% NaCl (S). Varying extents of cracking have developed in these columns due to AAR expansion. The columns half-immersed in salt solution over the past five years are contaminated with chloride and are prone to corrosion attack. These specimens are ideal for the study of the effects of CP current on corrosion mitigation in concrete containing reactive aggregate. Details of the columns are given in Table 1. Letters in the designations of the columns reflect the parameters mentioned above.

### **2.2 CP system**

In order to apply appropriate currents, the concrete resistivity was measured using a 4-pin resistivity meter. For the upper dry areas of columns, the resistivity was about 40 kΩ·cm. The lower wet parts of the columns, which were previously immersed in water or salt water, showed approximately 50% of this resistivity. The current supply was adjusted accordingly to provide the required current density.

A titanium mesh (Elgard 300 expanded mesh, MMO) was employed as the anode. Two separate pieces were wrapped around the upper and lower parts of the columns with a gap of about 20 mm. The wrapped areas were then patched with 10 mm thick mortar layer of 1: 3 (cement: sand), which filled the gap between the mesh and column surfaces, and formed a thin mortar layer over the mesh. Figure 2A shows the process for column 9, where the mesh has been fitted to the base of the column. Figure 2B shows the same

column after the mesh in the lower part has been embedded in mortar, and the mesh for the upper part been placed and is ready to be embedded.

After the anode installation, the columns were placed in plastic tubs and half-immersed in water. They were then connected to the power supply and the current distributed as illustrates in Figure 3, using impressed CP current levels of 5, 10 and 20 mA/m<sup>2</sup>, which cover the practical range of current density. Figure 4 shows the arrangement of columns and connection to power supply. The regulator board shown in Figure 4 allowed the current flowing to the top and bottom portions of the columns to be adjusted to the same values. Without this the current densities in these portions would have been different due to different concrete resistances in these zones. Before wrapping the columns with the anode mesh, the wet area of those columns previously stored in salt solution (Columns 6, 8 and 12) were tested for chloride content, half-cell potential and corrosion rate.

### 3 RESULTS

In the first phase of the research [13], some columns had developed various extents of cracking due to AAR. Corrosion of reinforcement had started in some of those stored in salt solution (Columns 6, 8 and 12), where rust staining was observed on the surface of the columns (mostly in lateral bars). This arose due to the penetration of chloride ions to the reinforcement level.

#### 3.1 Chloride profiles

The submerged parts of Columns 6, 8 and 12 were sampled for chloride profile analysis, and the results are presented in Figure 5. The profiles indicate that the threshold chloride content (0.4% by cement mass) has reached the reinforcing steel (main vertical bars at 50 mm, and lateral bars at 40-50 mm). This is in agreement with the observation of rust staining on the surface. The AAR cracking would have facilitated the corrosion and migration of rust to the surface, because companion columns without reactive aggregate did not produce any visual signs of corrosion despite having been stored in salt water [13].

#### 4.2 Half-cell potentials and corrosion rate of reinforcement before CP application

Half-cell potential values of the lower parts of the columns were measured prior to application of CP currents. An example of half-cell potential maps obtained is presented in Figure 6, which shows that the values were more negative than -350 mV CSE (copper-copper sulphate electrode potential), and indicates that reinforcement corrosion has started, in agreement with the observations made above. The corrosion rate of the steel bars was measured using linear polarisation technique, employing Gecor 6 which incorporates a guard ring to confine the area of steel for corrosion rate measurement. The corrosion rate was about 0.1 µA/cm<sup>2</sup>, which is categorised as “low corrosion rate”. The high alkali content of the columns (1.5 % by mass of cement) may have mitigated the corrosion rate of the reinforcing steel.

#### Polarization Potential Shift

Figure 7 shows an example of the polarisation, depolarisation curves obtained for Column 7. The instant-off potential was measured after 650 days of CP. When CP current was turned off, the potential of steel abruptly shifted to a more positive potential and then increased with time. When CP was turned on again, the potential shifted to the negative direction in a similar manner but the rate was faster (Figure 7). The depolarisation approached completion gradually, and appeared to become very slow after 5 hours. A depolarisation period of 4 hours or longer has been suggested as a reasonable time for monitoring the depolarisation [14].

The potentials of all the columns were measured between 5 - 6 hours after the CP current was turned off, and the values were taken as the potential shift. The potential shift was about 100 – 200 mV for

the lower part of columns; and 150 - 250 mV for the upper part of columns. The corroding steel bars showed a lower potential shift, e.g. Column 8, which has exhibited steel corrosion in the lower part, showed a potential shift of 155 mV and 247 mV for the lower and upper part, respectively. These potential shifts indicated that the CP system used provided adequate protection for most of the steel bars. Exceptions are the lower parts of Columns 7 and 9, which showed potential shift of only 60 mV.

### 3.2 Concrete expansion measurement

Concrete expansion was measured in four locations in each column, as designated below:

- TCC: Upper part and centre of column; strain gauge being installed perpendicular to column length.
- TCS: Upper part and surface of column; strain gauge being installed parallel to column length.
- BCC: Lower part and centre of column; strain gauge was installed perpendicular to column.
- BCS: Lower part and surface of column; strain gauge was installed parallel to column length.

Figures 8-13 show the full expansion results obtained over some 1600 days prior to application of CP (marked on the graphs), as well as data obtained over an additional 900 days after CP. Note that for column 10, BCC and BCS gauges failed at the age of 1653 days. At the start of the CP, concrete had expanded to about 1000-2500  $\mu\text{m}/\text{m}$ , depending on the aggregate type and early age curing history (Table 2). For the normal cured concrete (N), the expansion of concrete prior to the application of CP was approximately twice larger for the columns made with highly-reactive aggregate (Hr) compared with those made with low-reactive aggregate (Lr). The steam-cured columns made with (Lr) aggregate showed similar expansion as the columns made with (Hr) aggregate, subjected to normal curing. This means that the higher curing temperature compensated for the lower reactivity of the aggregate, and/or that some DEF-related expansion also occurred at high temperature.

The lower part of columns, which was immersed in water or salt solution, showed more expansion than the upper part. This was due to the availability of moisture, i.e. the upper part was in a semi-dry condition despite the efforts made to maintain the humidity by covering the columns and containers with plastic bags. The expansion of columns had generally slowed down after 2-3 years of exposure at 38°C, i.e., before the CP application, except for Column 5 and Column 6 which was continuing to expand at this stage. After the CP was applied, the expansion rate resumed and appeared to be at the same or higher rate than before the CP application, especially for the upper part of the columns. The extent of expansion depended on both the CP current density and the reactivity of the aggregate.

#### 3.2.1 Influence of CP density on the concrete expansion

As mentioned above, Column 5 and Column 6 exhibited the same rate of expansion before and after CP application. For other columns the expansion had reached a plateau before CP application, but exhibited increased expansion rate after CP. For example Column 8 (Figure 11) showed a high expansion rate for the lower part of the column (wet), but very low expansion for the upper part (drier) before the CP application. After the application of a high CP current (20 mA/m<sup>2</sup>), the upper part of this column started expanding at a significantly higher rate.

Column 9 (Figure 12) showed moderate expansion up to the age of about 1000 days, after which the expansion had reached a plateau up to 1600 days. After the application of a moderate CP current (10 mA/m<sup>2</sup>), the expansion rate increased again to the same rate as that before the age of 1000 days. One of the concrete gauges (TCC) in the upper part of this column showed a sudden increase in the expansion rate after about 1 year of CP, and its expansion was the highest in this column. The low CP current (5 mA/m<sup>2</sup>) also increased the expansion rate after the CP application, as shown by Column 12 (Figure 13).

Whereas the expansion curves would be expected to level off after several years under normal exposure conditions, the expansion curves show that the expansion increased under CP, and the rate of increase appears to be larger at higher CP current levels. The data was analysis to determine the expansion rate for the different currents, and the results are given in Table 3, indicating that the CP currents increased the AAR expansion.

The longer the period of CP application, the larger should be the increase in alkalinity, and the larger the recorded expansion. If sufficient data can be collected from the literature, then it may be possible to develop a relationship between the level of CP current and the resulting increase in AAR expansion.

#### 4 CONCLUSIONS

This work shows that application of CP current to AAR-affected reinforced concrete to suppress steel corrosion, can increase the AAR expansion. Higher current densities caused larger expansions. The following observations are made:

- The CP effect was more pronounced for the relatively dry part of concrete. This may be due to better supply of oxygen to the cathodic area.
- The expansion rate of concrete depended on aggregate reactivity, and CP current level. Additional expansion of 1000-2000  $\mu\text{S}$  were observed for both the slowly reactive aggregate subjected to 20 mA/m<sup>2</sup> and the highly reactive aggregate subjected to 10 mA/m<sup>2</sup> CP. The 5 mA/m<sup>2</sup> caused less expansion for the aggregates tested.

The results indicate that caution needs to be exercised to determine the AAR status of concrete, when application of impressed current CP is contemplated for protection of concrete structures at risk of corrosion damage.

#### 1 REFERENCES

- 1) Natesaiyer, K. and Hover, K.C. 1986. Investigation of electrical effects on alkali-aggregate reaction. Proceedings of the 7th ICAAR, Ottawa, Canada, pp. 466-471.
- 2) Sergi, G., Page, C.L. and Thompson, D.M. 1991. Electrochemical induction of alkali-silica reaction in concrete. Materials and Structures, Vol. 24, pp. 359-361.
- 3) Sergi, G. and Page, C.L. 1992. The effects of cathodic protection on alkali-silica reaction in reinforced concrete. TRRL Contract Report, No. 310, pp. 1-53.
- 4) Page, C.L., Sergi, G. and Thompson, D.M. 1992. Development of alkali-silica reaction in reinforced concrete subjected to cathodic protection. Proceedings of the 9th ICAAR, London, pp. 774-781.
- 5) Page, C.L. and Yu, S.W. 1995. Potential effects of electrochemical desalination of concrete on alkali-silica reaction. Magazine of Concrete Research. Vol. 47, (170), pp. 23-31.
- 6) Kuroda, T., Nishibayashi, S. and Bian, Q. 1996. Study of alkali-aggregate reactions in electrical fields. Proceedings of the 10th ICAAR, Melbourne, Australia, pp. 645-652
- 7) Ali, M.G. and Rasheeduzzafar. 1993. Cathodic protection current accelerates alkali-silica reaction. ACI Materials Journal May-June issue. Vol. 90, pp. 247-252.
- 8) Torii, K., Ishii, K. and Kawamura, M. 1997. Influence of cathodic protection on expansion and structural behaviour of RC beams containing alkali-reactive aggregates. East Asia AAR Seminar, Tottori (Japan), pp. 231-285.
- 9) Alkadhimi, T.K.H. and Banfill, P.F.G. 1996. The effects of electrochemical re-alkalisation on alkali-silica expansion in concrete. Proceedings of the 10th ICAAR, Melbourne, Australia, pp. 637-644.
- 10) Shayan, A., Janetzki, D. and Witt, P. 1998. Interaction of cathodic protection currents with AAR in concrete. Proceedings of the Australasian Corrosion Association Conference, Corrosion and Prevention 98, pp. 188-295..

- 11) Shayan, A., 2000. Combined effects of alkali-aggregate reaction (AAR) and cathodic protection currents in reinforced concrete. Proc. 11th Int. AAR Conf., June 2000, Quebec City, Canada, pp. 229-238.
- 12) Carse A. and Dux, P., 2004. An assessment of the risk of using a cathodic protection system on reinforced concrete piles where very reactive aggregates have been used. Proceedings of the 12th ICAAR, 15-19 Oct 2004, Beijing, China, pp 855-864.
- 13) Shayan, A., Xu, A. and Hii, A., 2006. Causes of deterioration of precast bridge piles: experimental study/Causes of deterioration of precast bridge piles and effect of repairs on columns. Proceedings of the 6th Austroads Bridge Conference., Perth, Western Australia, 14 pp.
- 14) Funahashi, M, and Bushmann, J.B 1991, „Technical review of 100 mV polarization shift criterion for reinforcing steel in concrete“, Corrosion, Vol.47, No.5, pp.376-385.

Table 1- Details of columns and applied CP current densities

Column	Mix No	Designation	Cl content (%)	CP current, (mA)	CP density, (mA/m <sup>2</sup> )
5	C04/997	Lr-N-W		1.5	5
6	C04/998	Lr-N-Salt	0.081	3.0	10
7	C04/1001	Lr-Ht-W		6.0	20
8	C04/1002	Lr-Ht-Salt	0.082	6.0	20
9	C04/1005	Hr-N-W		3.0	10
12	C04/1008	Hr-N-Salt	0.080	1.5	5

Table 2- Expansion of the concrete at the start of CP (µm/m)

Column	Top Centre	Top Side	Bottom Centre	Bottom Side
5 (Lr-N-W)	1290	920	1860	1560
6 (Lr-N-Salt)	800	726	1610	1610
7 (Lr-Ht-W)	1824	2035	4267	2190
8 (Lr-Ht-Salt)	470	570	2890	4490
9 (Hr-N-W)	1800	2420	2450	2850
12 (Hr-N-Salt)	1720	1650	2190	2650

Table 3- Expansion of concrete since imposing CP current (640 days)

Column	Top Centre (µm/m)	Top Side (µm/m)	Bottom Centre (µm/m)	Bottom Side (µm/m)	Average (µm/m)	Average rate (µm/m/day)
Column 5 (Lr-N-W), 5mA/m <sup>2</sup>	684	753	549	636	655	1.11
Column 12 (Hr-N-Salt), 5mA/m <sup>2</sup>	817	842	863	639	790	1.27
Column 6 (Lr-N-Salt), 10mA/m <sup>2</sup>	554	495	821	582	613	0.99
Column 9 (Hr-N-W), 10mA/m <sup>2</sup>	2684	803	1333	1064	1471 (1066 excl max.)	2.45 (1.47 excl max.)
Column 7 (Lr-Ht-W), 20mA/m <sup>2</sup>	1552	1172	258 at 59d	65 at 59d	1632	2.20
Column 8 (Lr-Ht-Salt), 20mA/m <sup>2</sup>	1100	1764	1295 at 419d	1060 at 419d	1432	2.61



Figure 1- Reinforcement configuration, and close up showing embedded concrete strain gauges

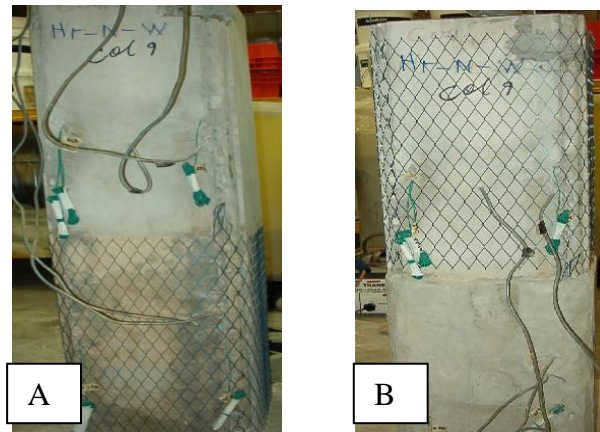


Figure 2- Installation of CP anode on the columns

**Concrete columns: Positions and applied current levels**

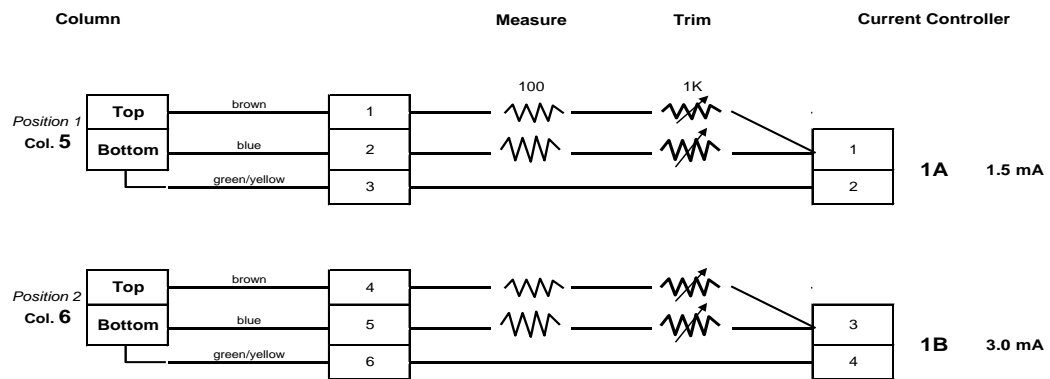


Figure 3- Examples of distribution of current by the power supply into two columns

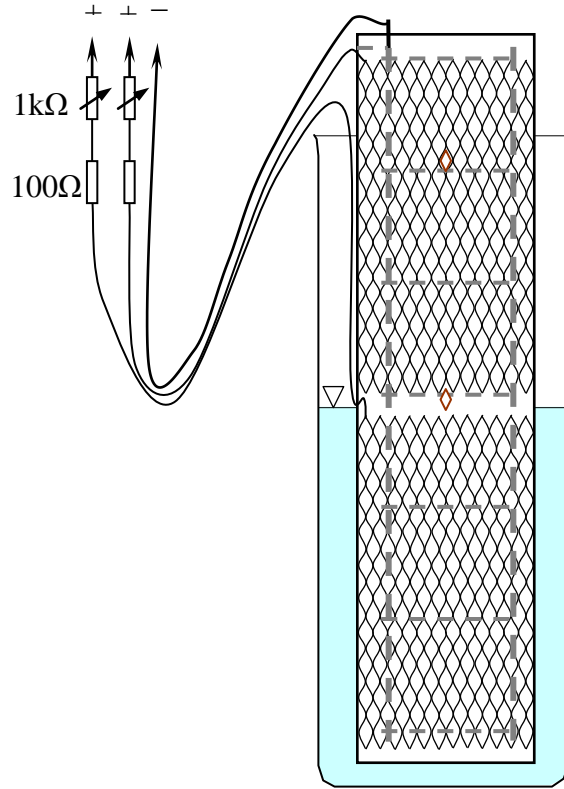
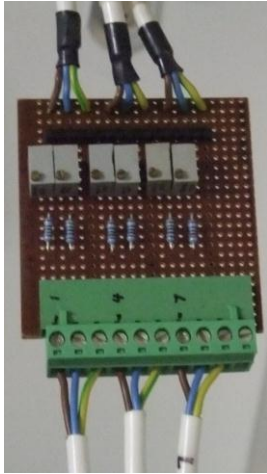


Figure 4- Left: Finished specimen connected to power supply (top), Current regulators for top and bottom parts of columns (bottom); Right: Arrangements for application of CP to column, +ve terminal to anode and -ve terminal to the reinforcement cage.

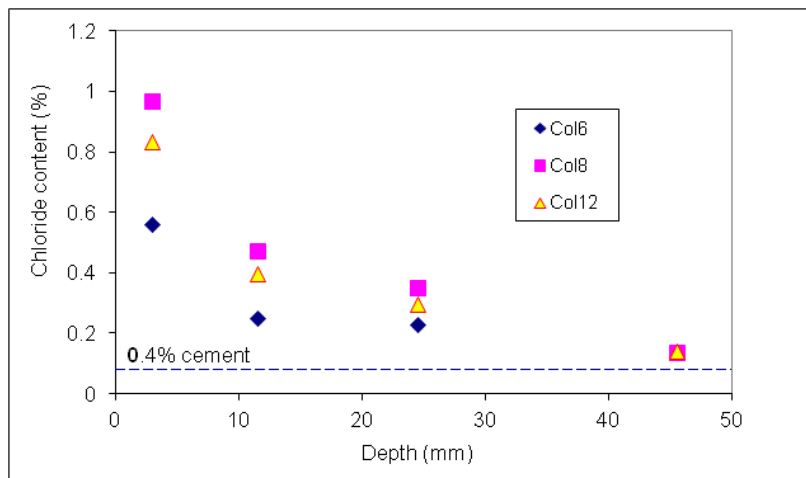


Figure 5- Chloride profiles for submerged portions of columns 6, 8 and 12



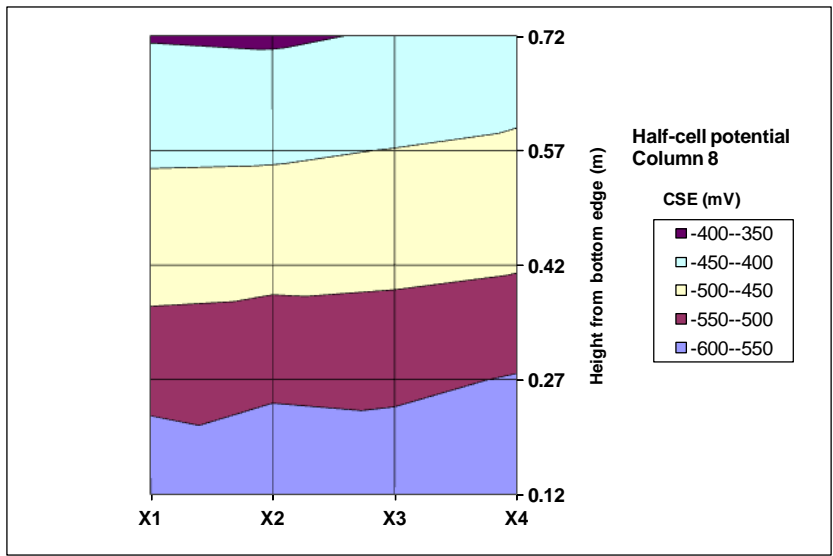


Figure 6- Half-cell potential map for the base of column 8, conducted on a 100 mm grid

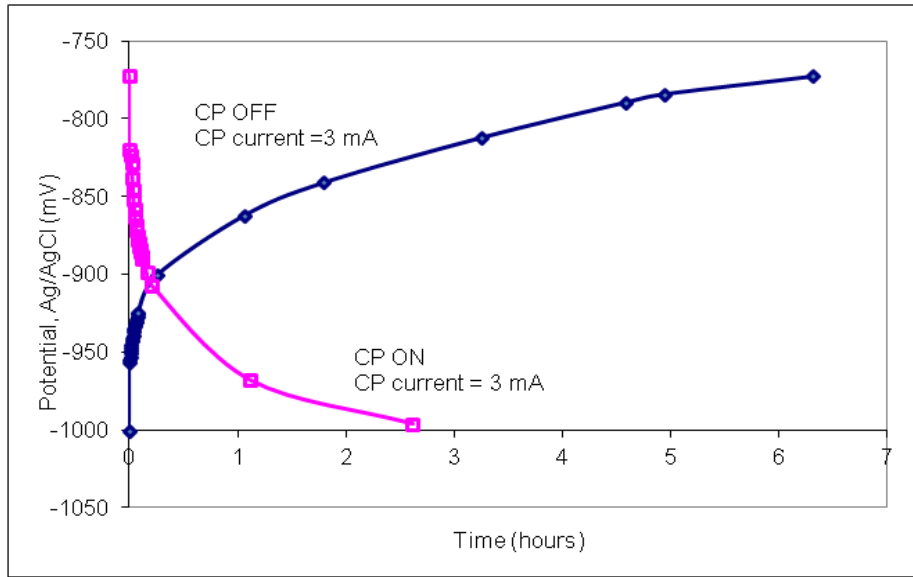


Figure.7- Potential changes of reinforcement during early period of CP OFF and CP ON, measured on upper part of Column 7 (CP current 3 mA; resistance between CP mesh and reinforcement was  $17\Omega$ )

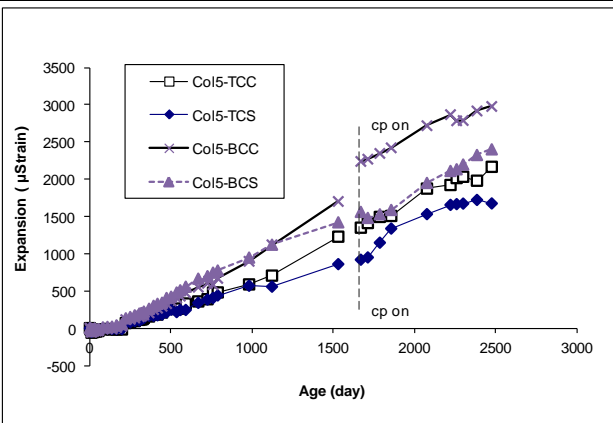


Figure 8- Column 5- Lr-N-W; CP current=5 mA/ m<sup>2</sup>

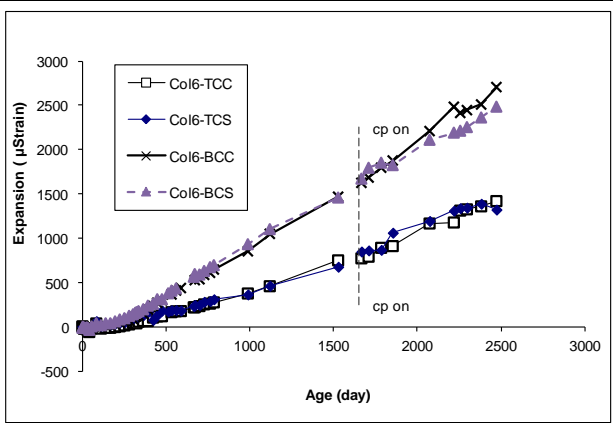


Figure 9- Column 6- Lr-N-Salt; CP current=10 mA/m<sup>2</sup>

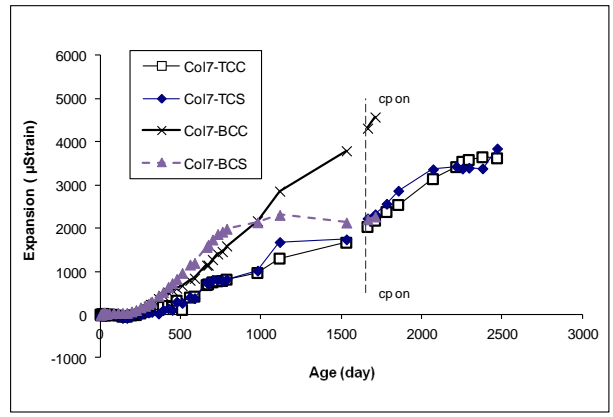


Figure 10- Column 7- Lr-Ht-W; CP current=20 mA/m<sup>2</sup>

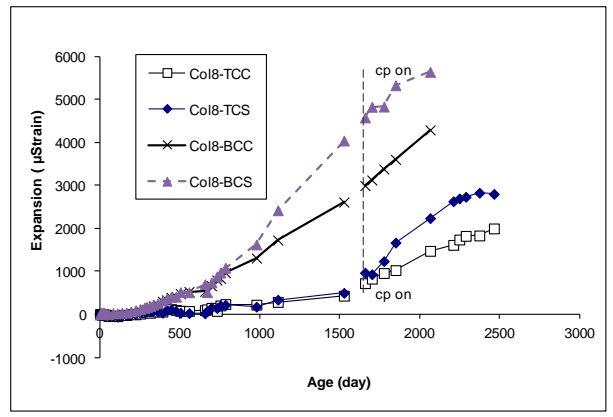


Figure 11- Column 8- Lr-Ht-Salt; CP current=20 mA/m<sup>2</sup>

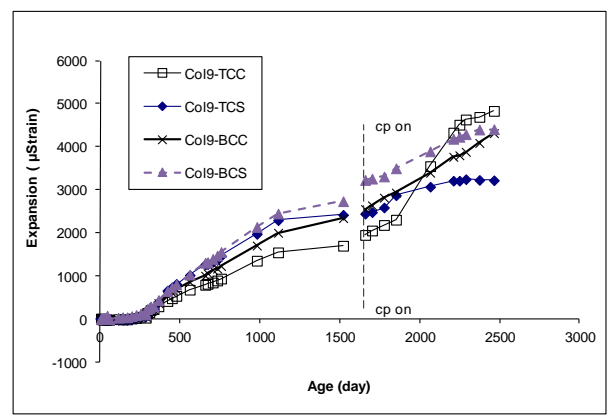


Figure 12- Column 9- Hr-N-W; CP current=10 mA/m<sup>2</sup>

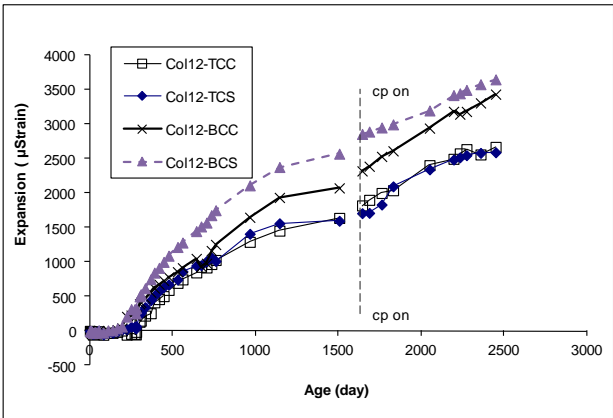


Figure 13- Column 12- Hr-N-Salt; CP current=5 mA/m<sup>2</sup>